

## Synthesis and characterization of Titanium dioxide nanorod by anodization and Sol-gel method

Jayaseelan R and Gopalakrishnan M\*.

Department of Chemistry, Annamalai University, Tamilnadu, India.

\*Corresponding Author: E-Mail: profmgk61@gmail.com

Received: 6<sup>th</sup> Dec 2016, Revised and Accepted: 8<sup>th</sup> Dec 2016

### ABSTRACT

A new Titania nanorod was prepared *via.*, alumina templates by adopting anodization process. The synthesis titanium nanorod was fully characterized by Scanning electron microscopy (SEM), powder X-ray diffraction, Raman spectroscopy, Brunauer-Emmett-Teller (BET), Transmission electron microscopy (TEM) and Energy-dispersive X-ray spectroscopy (EDX) analytical techniques. Energy-dispersive X-ray spectroscopy, VU-Visible spectroscopy and photoluminescence techniques were used to analyzed the prepared titanium Nanorod.

**Keywords:** TiO<sub>2</sub>; XRD; SEM; BET; TEM; EDX.

### 1. INTRODUCTION

In the present-day, nanostructured one-dimensional materials (1D) have been broadly studied due to their excellent geometries, novel chemical, physical properties, potential applications in nanoscale optical and electric devices [1-6]. TiO<sub>2</sub> with its different morphologies including nanoparticles, nanorods, nanotubes nano spheres, nanofibres and hollow have been explored for various applications. [7]. Nanostructured titanate nanorods also have been obtained in huge number and more attention due to their cheap fabrication, large surface area, pore volume, wide applications in photocatalysis, photovoltaic cells, catalytic supports and gas sensing. [8-16] Nanorod was prepared within confined spaces, such as porous alumina templates, have been reported. [17] economical process for directly creating TiO<sub>2</sub> with desired architectures is as importance but remains a key challenge for researchers [25-27].

### 2. Materials

Aluminium foil (99.9%) pure, ethanol, Perchloric acid (HClO<sub>4</sub>), Phosphoric acid, Chromic acid, sodium hydroxide and Titanium isopropoxide were purchased from sigma-aldrich. DC power supply From Agilent Company.

#### 2.1. Experimental Section

##### 2.1.1. Preparation of porous Aluminium template

A Size of glass slide Aluminium foil was sonicated for 10 minutes. Then it was allowed to electrophilishing about 10 min using electrolyte C<sub>2</sub>H<sub>5</sub>OH/H<sub>2</sub>O/ClHO<sub>4</sub> (67/13/20wt %) at P<sup>H</sup> 0.55 and 7°C, 20V, 1.00A in Agilent DC power supply. The substrate was anodizing in orthophosphoric acid (14wt %), electrolyte about 2.30 hrs by using 5.0V, 0.01A power supply. The electrolyte should have P<sup>H</sup> in the range 1.55 and Temp about 4°C. Then substrate was etching by mixture of Phosphoric acid (5.3wt %) and Chromic acid (1.7wt %). The same condition should be maintained for the second time anodization. Finally, the substrate was involved pore wiewing step by using 1M NaOH solution for 2 minits [28].

##### 2.1.2. Synthesis of Titanium nanorod

Titanium nanorod was prepared by sol-gel method. Aluminium template immersed in 3:1 ratio of Titanium isopropoxide and ethanol mixture. The sample was filtered by using vaccum filtration and dried at room temperature for 12 hrs. Then the prepared compound was calcinated at 500 °C. The resulting titanium nanorod was obtained.

### 3. RESULT AND DISCUSSION

#### 3.1. Scanning electron microscopy

The SEM observation of the compound showed dark and white spot, therefore, non uniformed pore was found. The SEM image of anodized aluminium foil is shown in figure 1. After the Pore wideing and etching of the Al foil SEM showed in figure 2 and 3 The pore size of

the Al foil template can be used to control the sizes, which typically range from 1 μm to 200 nm in diameter and several micrometers in length. The size of Titania is reduced to nanometer range to several micrometers in length. Apparently, the size distribution of the final TiO<sub>2</sub> nanorods is largely controlled by the size distribution of the pores of the Al foil templates were shown in Fig. 2,3. In order to obtain smaller and monosized TiO<sub>2</sub> nanorods, it is necessary to fabricate high-quality Al foil templates.

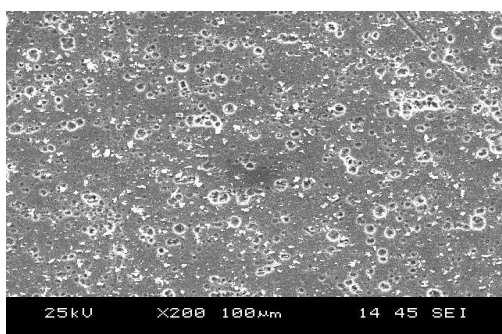


Figure - 1: Before Etching Al foil image.

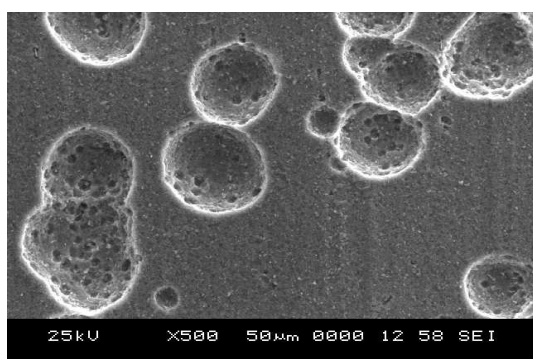


Figure - 2: After Etching image.

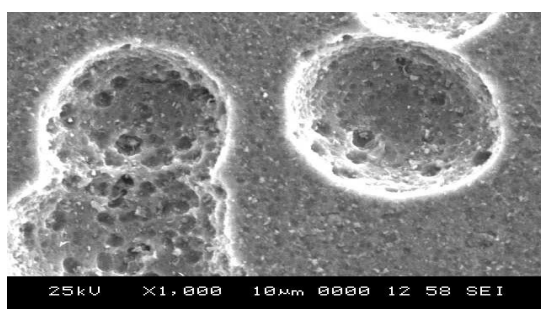


Figure - 3: After etching image.

### 3.2. X-ray diffraction pattern (XRD) of TiO<sub>2</sub>

The experimental powder X-ray diffraction Pattern as synthesized Titanium dioxide (TiO<sub>2</sub>) nanorod is presented in figure 4. Shown some intensively well defined diffraction peaks at angles 18.63, 25.13, 32.45, 36.94, 37.79, 38.56, 44.25, 47.52, 52.51, 52.91, 53.96 and 71.23 compounds to the diffraction plans (002), (101), (110), (103), (004), (112), (113), (200), (202) and (114) with relative intensities of about

7, 100, 43, 6, 3, 5, 5, 6, 7, and 7% respectively. The observed XRD peaks are very distinct and discrete which are shown the crystalline nature of as-synthesised titanium dioxide nanoparticles and the crystalline size were calculated by using the schennar equation, here some peaks observed 32.45 and 71.23 compounds to the diffraction plans (111) and (311), it conformed present in Al peaks. Therefore only TiO<sub>2</sub> and Al peaks are observed, other crystalline impurities are not observed.

$$\tau = \frac{K\lambda}{\beta \cos\theta}$$

Where  $\tau$  The partial of size

K, Shape factor,(0.89)

$\lambda$ , Wave length of the X-ray used

B, Full width of half maxima(FWHM)

$\theta$ , Bragg's angle.

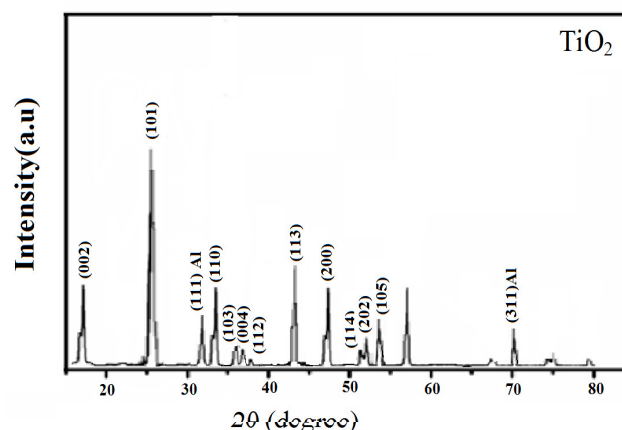


Figure - 4: XRD pattern of TiO<sub>2</sub> Nanorod.

The estimated particle sizes were found to be in the range of 50-100 nm. As seen in the **Table 1**, the obtained experimental result was comparable to that of the standard references XRD pattern of the title compound having a tetragonal symmetry [JCPDS ID: 89-4203] with space group of P<sub>4</sub><sub>2</sub>/mm. The tetragonal cell parameter were found to be 407 and 2.8 Å

### 3.3 Raman spectroscopy of TiO<sub>2</sub>

Raman spectroscopy is an effective technique, for the analysis of different phases of TiO<sub>2</sub>. Above the calibration of the maximum low frequency band, it is possible to find out the nanoparticle size shown in the **Fig. 5**. From the group analysis, anatase have six active Raman modes, (A<sub>1g</sub> + 2B<sub>1g</sub> + 3E<sub>g</sub>), antase single crystal have been investigated by Ohsaka, ]. The observed peakes of bulk anatase appears at 145.9 cm<sup>-1</sup> (E<sub>g</sub>), 197 cm<sup>-1</sup> (E<sub>g</sub>), 441.5cm<sup>-1</sup> (B<sub>1g</sub>), and at 612.3 cm<sup>-1</sup> (E<sub>g</sub>) [28 & 29]. Raman spectra of commercially available

anatase microcrystalline samples are reported for comparison

**Table - 1: Experimental powder XRD pattern of TiO<sub>2</sub> nanoparticles**

| 2Theta (°) | Intensity(a.u) | Diffraction plane (h k l) |
|------------|----------------|---------------------------|
| 18.63      | 65             | 0 0 2                     |
| 25.13      | 999            | 1 0 1                     |
| 32.45      | 430            | 1 1 0                     |
| 33.86      | 480            | 1 1 1                     |
| 36.94      | 55             | 1 0 3                     |
| 37.79      | 45             | 0 0 4                     |
| 38.56      | 10             | 1 1 2                     |
| 44.25      | 125            | 1 1 3                     |
| 47.52      | 146            | 2 0 0                     |
| 52.51      | 25             | 1 1 4                     |
| 52.91      | 32             | 2 0 2                     |
| 53.96      | 39             | 1 0 5                     |
| 71.23      | 90             | 3 1 1                     |

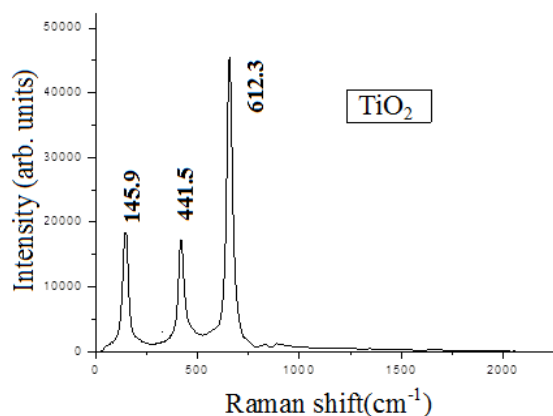


**Figure - 5: Raman spectra of TiO<sub>2</sub> nanorod.**

### 3.4. The BET surface area

BET surface area of the as-prepared TiO<sub>2</sub> nanorod samples surface area is found to be 67 m<sup>2</sup>/g. TiO<sub>2</sub> nanorod sample was checked by Nitrogen adsorption/ desorption isotherm and the pore size distribution were calculated by Barrette-Joyner- Halenda (BJH) show in figure 6.

The BET specific surface area was determined by multipoint BET method using adsorption data and answering pore size distribution curves of TiO<sub>2</sub> nanorods.[30] First sample was degasing at 170 °C for 2 hours then the sample involved in isotherms and pore distribution. The TiO<sub>2</sub> nanorod has isotherm relative pressure range 0.7-1.0, point out the nanorod mesopores (2-50nm). Further the observed hysteresis loop approaches relative pressure (P/P<sub>0</sub>). The pore volume of the TiO<sub>2</sub>

nanorod prepared at R<sub>TiO<sub>2</sub></sub> = 0.6 are 0.95 and 0.25cm<sup>3</sup>/g. In fact, the nanorod does not have macropores and mesopores. The TiO<sub>2</sub> nanorods are existing in nanopore size. Therefore specific pore volume and surface area increase, while there is little decrease in average pore due to the suppression of crystalline growth.

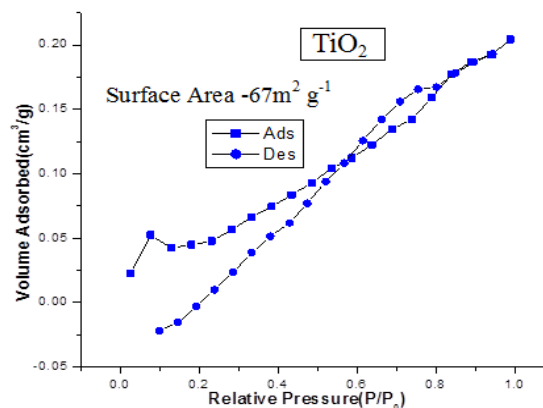


**Figure - 6: TiO<sub>2</sub> nanorod surface area.**

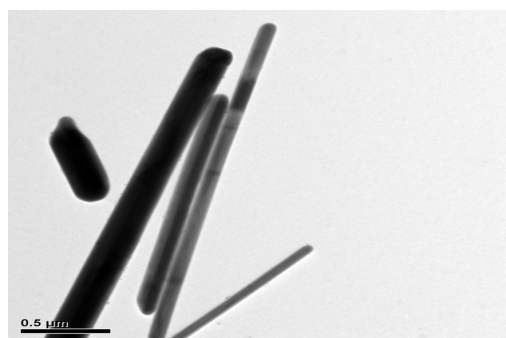


**Figure - 7: TEM image of TiO<sub>2</sub> nanorod.**

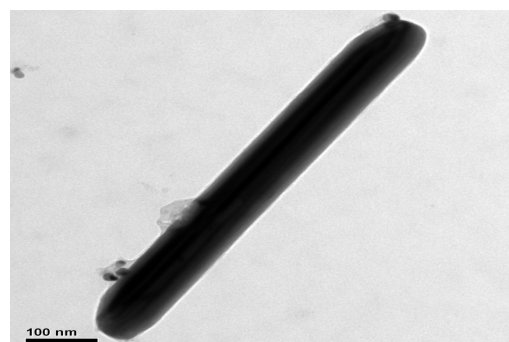


**Figure - 8: TEM image of TiO<sub>2</sub> nanorod.**

### 3.5. Transmission electron microscopy (TEM)

The calcination of Titanium dioxide nanorod can be familiar to control, the crystalline phase compare with all other phase anatase obtained at low temperature. Anatase TiO<sub>2</sub> nanorods morphology image is shown below figure 7-8. Chemically synthesized anatase TiO<sub>2</sub> nanorods have a length and diameter in the range ~100nm- 0.5μm. The high resolution scanning transmission electron microscopy at higher magnification lattice can be done nanocrystals

oriented to exist, it planes, anatase phase crystalline nanorod coexisting with alone observable TiO<sub>2</sub> nanorods. The selected area of electron distribution pattern shows bright dots, indicating that TiO<sub>2</sub> is crystalline in nature shows in Fig.9. It was derived from electron beam. We strongly agree with the nanocrystal identifies the sample as anatase [31-32].

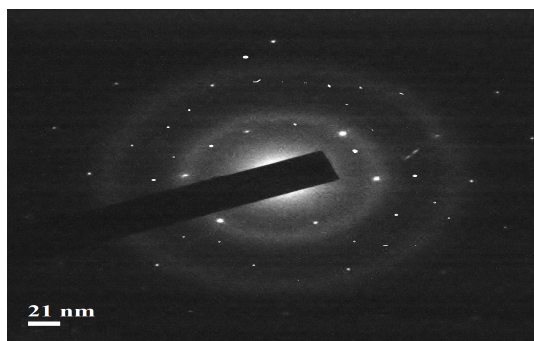


Figure - 9: SAED image of TiO<sub>2</sub> nanorod.

Selected area (electron diffraction) is another technique of crystallographics; It was fixed in transmission electron microscopy. TiO<sub>2</sub> gives d-value of 0.372 (d-value find in different phases in literature) correspond to (101), plane of anatase TiO<sub>2</sub> [33].

### 3.6. Energy dispersive x-ray spectroscopy

The feature of all EDX analyses of the titanium dioxide is found to be presented in EDX only Al, Ti and O (see Fig. 10). The peak obtained as sharp and well visible in this figure. Here predominantly Ti, and O peaks were very clearly identified, and while Al peak due to Aluminium foil by using anodization, also observed.

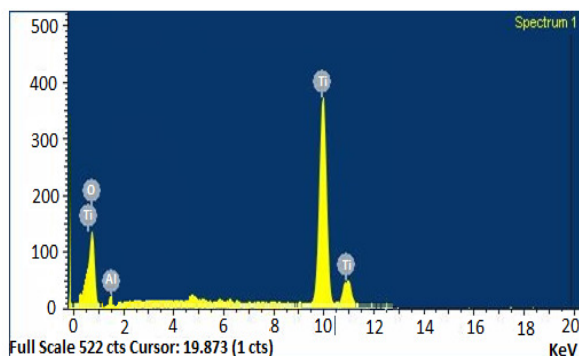


Figure - 10: EDX of TiO<sub>2</sub>.

### 3.7. UV- Visible spectroscopic analysis

Titanium nanorod f obtained at ordinary temperature UV-Visible absorption spectrum of sol-gel synthesized TiO<sub>2</sub> appeared in the range of 200 to 700nm wavelength shown in the figure 11. There is a significant increase in absorbtion of TiO<sub>2</sub> in the range of 373nm [33,35] in the visible region.

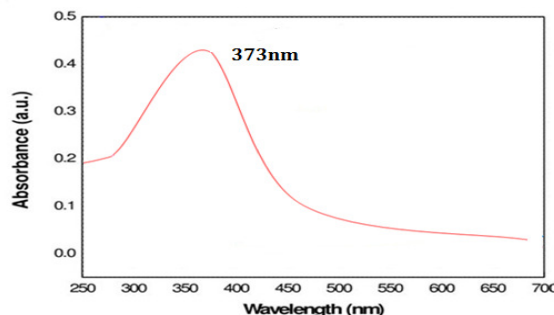


Figure - 11: UV-Visible absorption spectram of TiO<sub>2</sub>.

The band gap energy of TiO<sub>2</sub> Hence, by using Kubelk-Munk equation for band gap energy shows figure 12.

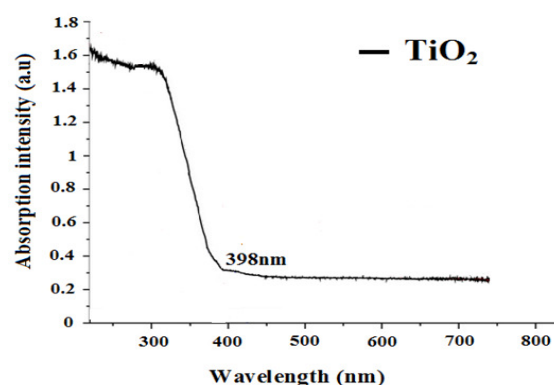


Figure - 12: Kubelk-Munk Absorption visible spectra.

So, using Kubelk-Munk equation

$$F(R)E^2 = \left[ \frac{(1-R)^2}{2R} \right]^{1/2}$$

The resulting band gap energy of TiO<sub>2</sub> is 3.2eV. Therefore, band gap energy reduce, so, it act as good photocatalyst activity

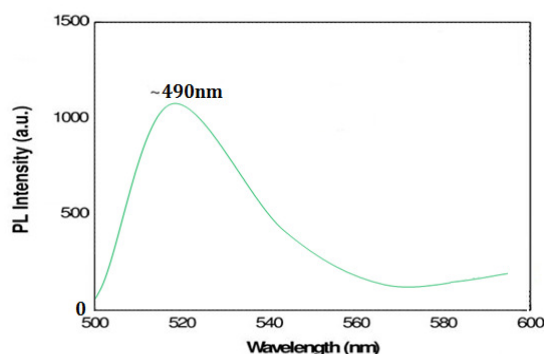


Figure - 13: Photoluminescence image of TiO<sub>2</sub>.

### 3.8. Photoluminescence

Photoluminsence of our data shown in the Fig.13, it is of consist and clarification, that the extraordinary optical band gap was controlled by B titanium nanorods. Therefore this phenomenon

displaying its very great optical quality is in great agreement with that reported value by other researchers<sup>[34]</sup>.

#### 4. CONCLUSION

In summary, a facile was developed for the growth of single-crystalline Anatase TiO<sub>2</sub> nanorod with various aspect were synthesized by Anodization Aluminium Oxide, Sol-gel method and size controlled were generated. A wide range of particle is size particularly 100nm-5 $\mu$ . It may be used the great Anti-bacterial activity and photocatalytic activity. The growth parameters like growth time, growth temperature and the initial reactant concentration. As evidence from TEM, Titania partical size is in the range from ~50nm- 0.2 $\mu$ m. A short synthesizing process and low reaction temperature. Sol-gel method is used reduce the possibility of the particle growth and besides, Morphology evolution were studied various characterization techniques such as XRD, SEM, and TEM. This UV-Visible, Photoluminescence studies potentially can be used to improve optical properties.

#### 5. REFERENCES

- H. Tokudome, M. Miyauchi, Chem. Commun. (2004) 958.
- J.G. Yu, J.C. Yu, W.K. Ho, L. Wu, X.C. Wang, J. Am. Chem. Soc. 126 (2004) 3422.
- X.M. Sun, Y.D. Li, Chem. Eur. J. 9 (2003) 2229.
- J.G. Yu, F.-R.F. Fan, S.L. Pan, V.M. Lynch, K.M. Omer, A.L. Bard, J. Am. Chem. Soc. 130 (2004) 7196.
- G.H. Du, Q. Chen, R.C. Che, Z.Y. Yuan, L.P. Peng, Appl. Phys. Lett. 79 (2001) 3702.
- J.G. Yu, M.H. Zhou, Nanotechnology 19 (2008) 045606.
- Tian Yuan, Li Zhao, Hongbing Lu, Li Wan, Binghai Dong, Shimin Wang, Zuxun Xu, "Single-crystalline rutile TiO<sub>2</sub> nanorod arrays with high surface area for enhanced conversion efficiency in dye-sensitized solar cells," J Mater Sci: Mater., vol. 26, pp. 1332-1337, January 2015.
- J.G. Yu, H.G. Yu, B. Cheng, X.J. Zhao, Q.J. Zhang, J. Photochem. Photobiol. A 182 (2006) 121.
- W.J. Dong, A. Cogbill, T.R. Zhang, S. Ghosh, Z.R. Tian, J. Phys. Chem. B 110 (2006) 16819.
- T. Kasuga, M. Hiramatsu, A. Hoson, T. Sekino, K. Niihara, Langmuir 14 (1998) 3160.
- G.S. Kim, H.K. Seo, V.P. Godble, Y.S. Kim, O.B. Yang, H.S. Shin, Electrochem. Commun. 8 (2006) 961.
- H. Tokudome, M. Miyauchi, Angew. Chem. Int. Ed. 44 (2005) 1974.
- R.R. Tian, J.A. Voigt, J. Liu, B. McKenzie, H.F. Xu, J. Am. Chem. Soc. 125 (2003) 12384.
- H.G. Yu, J.G. Yu, B. Cheng, S.W. Liu, Nanotechnology 18 (2007) 065604.
- T. Kasuga, M. Hiramatsu, A. Hoson, T. Sekino, K. Niihara, Adv. Mater. 11 (1999) 1307.
- M. Miyauchi, H. Tokudome, Thin Solid Films 515 (2006) 2091.
- Woo Lee, Roland Scholz and Ulrich Gösele, Nano Lett., 2008, 8 (8), pp 2155-2160
- Remskar, M. Adv. Mater. 2004, 16, 1497.
- Maca'k, J. M.; Tsuchiya, H.; Taveira, L.; Aldabergerova, S.; Schmuki, P. Angew. Chem., Int. Ed. 2005, 44, 7463.
- Patzke, G. R.; Krumeich, F.; Nesper, R. Angew. Chem., Int. Ed. 2002, 41, 2446.
- Guiju Liu, Yiqian Wang, Bin Zou, Wenshuang Liang, Neil McN. Alford, David W. McComb, and Peter K. Petrov; 10.1021/acs.jpcc.6b03833, 2016
- Jan Torgersen, Shinjita Acharya, Anup Lal Dadlani, Ioannis Petousis, Yongmin Kim, Orlando Trejo, Dennis Nordlund, and Fritz B. Prinz J. Phys. Chem. Lett. 2016, 7, 1428-1433
- Alexander A. Semenov<sup>1</sup>, Antonina I. Dedyk<sup>1</sup>, Andrey A. Nikitin<sup>1</sup>, Pavel Yu. Belyavskiy<sup>1</sup>, Yulia V. Pavlova<sup>1</sup>, Ivan L. Mylnikov<sup>1</sup>, Alexey B. Ustinov<sup>1</sup>, Viktor V. Plotnikov<sup>2</sup>, Andrey V. Eskov<sup>2</sup>, Oleg V. Pakhomov<sup>2</sup>, and Andrey A. Stashkevich<sup>3,2</sup> J Mater Sci (2016) 51:7803-7813
- Maria A. Gomes, A 'lvaro, S. Lima<sup>1</sup> Katlin I. B. Eguiluz<sup>1</sup>, Giancarlo R. Salazar-Banda<sup>1</sup> , J Mater Sci (2016) 51:4709-4727.
- Jun Su<sup>1</sup>, Jun Zhang<sup>1</sup> , J Mater Sci: Mater Electron (2016) 27:4344-4350.
- Mehrnoush Nakhaei<sup>1</sup>, Ali Bahari<sup>1</sup> J Mater Sci: Mater Electron (2016) 27:5899-5908.
- Marin Cernea, Catalina Andreea Vasilescu, Mihail Secu<sup>1</sup>, Gheorghe Aldica, Adrian 42 (1983) 3312.Surdu, Paul Ganea<sup>1</sup> J Mater Sci: Mater Electron 10.1007/s10854-016-5262-2
- T. Ohsaka, J. Phys. Soc. Jpn. 48 (1980) 1661.
- M.A. Marcus, M.P. Andrews, J. Zegenhagen, A.S. Bommannavar, P. Montano, Phys. Rev. B
- G.D. Sulka, S. Stroobants, V. Moshchalkov, G. Borghs, J.P. Celis, Journal of The Electrochemical Society, 149 -7! D97-D103 - 2002.

31. S. Brunauer, P. H. Emmett and E. Teller, *J. Am. Chem. Soc.*, 1938, 60, 309. doi:10.1021/ja01269a023.
32. Mohammad Rehan, Xiaojun Lai and Girish M. Kaleb, Hydrothermal synthesis of titanium dioxide nanoparticles studied employing in situ energy dispersive X-ray diffraction, DOI:10.1039/c0ce00781a
33. Wonjun Kang, Charles S. Spanjers, Robert M. Rioux and James D. Hoefelmeyer Synthesis of brookite TiO<sub>2</sub> nanorods with isolated Co(II) surface sites and photocatalytic degradation of 5,8-dihydroxy-1,4-naphthoquinone dye : 10.1039/c3ta11038a
34. LI Yue-Jun, CAO Tie-Ping, MEI Ze-Min, Preparation and Photocatalytic Properties of BaTiO<sub>3</sub>/TiO<sub>2</sub>Heterostructured Nanofibers, 1000-324X(2014)07-0741-06, 43
35. Vandana Kumari, Manickam Sasidharan and Asim Bhaumik *Dalton Trans.*, 2015,44, 1924-1932 DOI: 10.1039/C4DT03180F,44.
36. M.R.A. Bhuiyan, M.M. Alam, M.A. Momin, M.J. Uddin , M.Islam Synthesis and Characterization of Barium Titanate (BaTiO<sub>3</sub>) Nanoparticle, *International Journal of Material and Mechanical Engineering*, 2012, 1: 21-24,45